

CRRES Observations of the Composition of the Ring-Current Ion Populations

15 February 1995

Prepared by

J. L. ROEDER, J. F. FENNELL, and M. W. CHEN
Space and Environment Technology Center
Technology Operations
The Aerospace Corporation

M. SCHULZ
Lockheed Palo Alto Research Laboratory

M. GRANDE
Rutherford Appleton Laboratory

S. LIVI
Max-Planck-Institute for Aeronomy

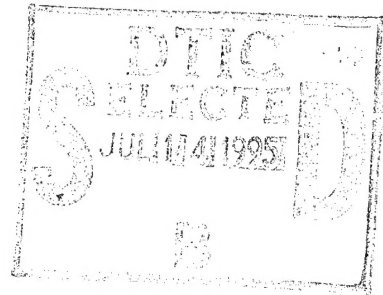
DTIC QUALITY INSPECTED 5

Prepared for

SPACE AND MISSILE SYSTEMS CENTER
AIR FORCE MATERIEL COMMAND
2430 E. El Segundo Boulevard
Los Angeles Air Force Base, CA 90245

Engineering and Technology Group

19950710 049

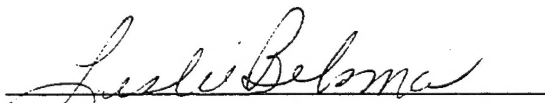


APPROVED FOR PUBLIC RELEASE;
DISTRIBUTION UNLIMITED

This report was submitted by The Aerospace Corporation, El Segundo, CA 90245-4691, under Contract No. F04701-93-C-0094 with the Space and Missile Systems Center, 2430 E. El Segundo Blvd., Los Angeles Air Force Base, CA 90245. It was reviewed and approved for The Aerospace Corporation by A. B Christensen, Principal Director, Space and Environment Technology Center.

This report has been reviewed by the Public Affairs Office (PAS) and is releasable to the National Technical Information Service (NTIS). At NTIS, it will be available to the general public, including foreign nationals.

This technical report has been reviewed and is approved for publication. Publication of this report does not constitute Air Force approval of the report's findings or conclusions. It is published only for the exchange and stimulation of ideas.


Leslie Belsma, Maj. USAF
SMC/IMO

REPORT DOCUMENTATION PAGE			Form Approved OMB No. 0704-0188	
Public reporting burden for this collection of information is estimated to average 1 hour per response, including the time for reviewing instructions, searching existing data sources, gathering and maintaining the data needed, and completing and reviewing the collection of information. Send comments regarding this burden estimate or any other aspect of this collection of information, including suggestions for reducing this burden to Washington Headquarters Services, Directorate for Information Operations and Reports, 1215 Jefferson Davis Highway, Suite 1204, Arlington, VA 22202-4302, and to the Office of Management and Budget, Paperwork Reduction Project (0704-0188), Washington, DC 20503.				
1. AGENCY USE ONLY (Leave blank)		2. REPORT DATE 15 February 1995		3. REPORT TYPE AND DATES COVERED
4. TITLE AND SUBTITLE CRRES Observations of the Composition of the Ring-Current Ion Populations			5. FUNDING NUMBERS F04701-93-C-0094	
6. AUTHOR(S) J. L. Roeder, J. F. Fennell, M. W. Chen, M. Schulz, M. Grande, and S. Livi				
7. PERFORMING ORGANIZATION NAME(S) AND ADDRESS(ES) The Aerospace Corporation Technology Operations El Segundo, CA 90245-4691			8. PERFORMING ORGANIZATION REPORT NUMBER TR-95(5940)-3	
9. SPONSORING/MONITORING AGENCY NAME(S) AND ADDRESS(ES) Space and Missile Systems Center Air Force Materiel Command 2430 E. El Segundo Boulevard Los Angeles Air Force Base, CA 90245			10. SPONSORING/MONITORING AGENCY REPORT NUMBER SMC-TR-95-25	
11. SUPPLEMENTARY NOTES				
12a. DISTRIBUTION/AVAILABILITY STATEMENT Approved for public release; distribution unlimited			12b. DISTRIBUTION CODE	
13. ABSTRACT (Maximum 200 words) The Magnetospheric Ion Composition Spectrometer onboard the CRRES spacecraft provided mass and charge state composition data for positive ions in the energy-per-charge range 10–425 keV/e. The CRRES data is compared to the AMPTE/CCE observations during both geomagnetically quiet and active periods. The CRRES average radial profiles of H ⁺ , He ⁺ , and He ⁺⁺ during quiet intervals are remarkably similar to those measured by CCE. The excess of ions measured by CRRES at L < 4 compared to standard ion transport models tends to support the necessity of additional ion radial diffusion by ionospheric electric-field variations. A summary is also given of the measured storm-time variations of the major ion populations during the large storm of March 1991. The results are compared to previous observations by the AMPTE/CCE spacecraft during a large storm. The CRRES data confirm that the rapid initial recovery of the Dst magnetic index is due to a momentary change of the relative ion composition of the ring current to an oxygen-dominated state. A preliminary test of the Dessler-Parker-Sckopke relation between the ion energy and the global magnetic perturbation shows that the observed particle fluxes during the March 1991 storm could account for only 30–50% of the variation of the Dst magnetic index.				
14. SUBJECT TERMS Magnetosphere, ring current, trapped particles			15. NUMBER OF PAGES 14	
			16. PRICE CODE	
17. SECURITY CLASSIFICATION OF REPORT UNCLASSIFIED	18. SECURITY CLASSIFICATION OF THIS PAGE UNCLASSIFIED	19. SECURITY CLASSIFICATION OF ABSTRACT UNCLASSIFIED	20. LIMITATION OF ABSTRACT	

Preface

We would like to thank H. J. Singer for making available the magnetometer data from the CRRES spacecraft. Work performed at The Aerospace Corporation was supported by the US Air Force System Command's Space Systems Division under contract F04701-91-C-0089 and by the Aerospace Sponsored Research program. Work performed at Lockheed was supported by the company's Independent Research and Development (IR&D) program. The MICS sensor was provided by a team from the Max-Planck-Institute for Aeronomy, with support from the Max-Planck-Gesellschaft zur Förderung der Wissenschaften, the Rutherford Appleton Laboratory, and the University of Bergen.

Accession For	
NTIS GRA&I	<input checked="checked" type="checkbox"/>
DTIC TAB	<input type="checkbox"/>
Unannounced	<input type="checkbox"/>
Justification	
By	
Distribution	
Availability Codes	
Dist	Avail and/or Special
A-1	

Contents

Introduction	1
Observations.....	3
Average Ion Populations During Geomagnetically Quiet Intervals.....	3
Storm-Time Variations of Ion Composition.....	6
Conclusions.....	11
References.....	13

Figures

1. Equatorial radial phase-space density profiles for trapped protons during quiet times at four values of magnetic moment.....	4
2. Quiet-time radial profiles of the He^{++} phase-space density at two values of magnetic moment from CRRES and CCE measurements and the standard transport model.....	5
3. Quiet-time radial profiles of the He^+ phase-space density at four values of magnetic moment from CRRES and CCE measurements and the standard transport model.....	6
4. Total ion energy density for $L = 3$ to 5 for the four major ion species in the energy range 40–426 keV compared with the variation of the magnetic index Dst during the large geomagnetic storm on 23 March 1991.....	7

Introduction

Variations of the populations of 1–500 keV ions in the magnetosphere known as the ring current can have global effects on the magnetic field even at ground level. Many early efforts were made to measure these particles without explicit composition information /1,2/. Those studies had assumed that the ion populations consisted mainly of protons. More recent missions have included time-of-flight spectrometers that measure ion composition in the energy range that contributes the bulk of the ring current. For example, in a complete study of one moderate storm based on data from the AMPTE Charge Composition Explorer (CCE) spacecraft /3,4,5/, protons were found to have dominated the composition of the ring current, while the heavier ions played only a negligible role.

Hamilton and Gloeckler studied a large storm using CCE data and concluded that oxygen ions became the dominant contributor to the particle energy content of the ring current during the peak of the main phase /6/. They compared the evolution of the relative composition with the variation of the *Dst* index. They concluded that the so-called two-phase recovery of *Dst* is due to a change in composition from proton to oxygen dominance. By this interpretation, the initial rapid recovery of *Dst* was caused by the fast loss of O^+ through charge exchange. The slower decay of *Dst* later in the recovery phase is attributed to the longer charge exchange lifetime of H^+ . The idea that the relative ion composition could drastically alter the decay rate of the ring current was first proposed by Tinsley /7/, who attempted to explain the anomalously long particle lifetimes observed in recovery phase /8/ as a consequence of a helium-dominated plasma. Later analysis of the CCE ion composition data /6/ provided the first experimental test of this concept, but with oxygen ions substituted for helium. As we note below, this theory still does not explain the two-stage signature in the *Dst* variation during some moderate intensity storms that are dominated by hydrogen ions. For example, the *Dst* variation (reaching only to -124 nT) during the September 1984 storm studied by the CCE group shows a clear two-stage recovery feature /3/.

Significant ion populations are present even during geomagnetically quiet intervals. These contribute to the baseline of *Dst*, which is used as a reference for stormtime deviations. The quiet-time populations are very important theoretically because they serve as initial conditions for dynamic models of the storm-time enhancement of the ring current. Sheldon and Hamilton /9/ and Sheldon /10/ described a study in which many orbits of AMPTE/CCE data were combined to produce average equatorially mirroring hydrogen and helium ion phase-space distributions as functions of magnetic moment and *L* shell. These distributions were then compared to a standard model of ion transport /11/ that included radial diffusion by fluctuating convection electric fields, charge exchange, and Coulomb drag. Sheldon and Hamilton /9/ found a significant deficit in the model ion fluxes on the lower *L* shells as compared to the observations. Sheldon /10/ showed that this discrepancy could be explained by including in the model an enhanced radial diffusion due to ionospheric electric-field variations that have been mapped upward into the magnetosphere.

In this paper, we give a summary of our results from the Magnetospheric Ion Composition Spectrometer (MICS) on the Combined Release and Radiation Effects Satellite (CRRES). This includes observations of ring-current ion populations during both geomagnetically quiet and

geomagnetically active intervals. We focus on comparing the CRRES solar maximum observations with previous measurements performed by the AMPTE/CCE spacecraft near solar minimum.

Observations

The CRRES spacecraft was launched on 25 July 1990 into a geosynchronous transfer orbit of dimensions $350 \text{ km} \times 33,584 \text{ km}$ and 18.1° inclination [12]. The satellite operated nominally until a battery failure ended the mission on 14 October 1991, so that the usable data thus span 1065 orbits. The magnetic local time of apogee ranged from 8.4 hr just after orbit insertion to approximately 14 hr at the end of mission. Observations reported in this paper were taken by the Magnetospheric Ion Composition Spectrometer (MICS). This instrument uses an electrostatic analyzer, a time-of-flight chamber, and a solid-state detector to measure the mass, energy, and charge state of particles with energies in the 1–430 keV/charge range. A more detailed description of the sensor and its data processing unit is given in other papers [13,14].

Average Ion Populations During Geomagnetically Quiet Intervals

An analysis of the ion populations for geomagnetically quiet intervals has been performed using the CRRES MICS data. Hourly intervals for analysis were selected by using criteria on Kp and Dst identical to those used in a similar study by Sheldon and Hamilton [9]. The criteria are as follows: (1) $|Dst| < 11 \text{ nT}$ for every hour included; (2) $|Dst| < 16 \text{ nT}$ for 24 hours preceding every hour included; (3) $Kp < 2+$ for every hour included; and (4) $Kp < 3$ for 24 hours preceding every hour included. The ion fluxes of local pitch angle in the range 70 – 110° were averaged in L -shell bins of width $\delta L = 0.5$, and with centroids in the range $L = 3$ to 7 . The analysis was also restricted to the region near the geomagnetic equator by rejecting all bins in which B/B_0 (\equiv ratio of measured B-field magnitude to the model field minimum at the same L) was greater than 1.2. The 1977 Olsen-Pfitzer model of the geomagnetic field was used to calculate the L values and field minima. It is assumed here that during quiet intervals the local-time variations in the ion distributions are so small that the phase-space densities f from all local times at each L shell can be averaged together to construct f as a function of magnetic moment. For nonrelativistic ions, the magnetic moment μ is equal to the first adiabatic invariant of charged-particle motion. This quantity should organize the data well if the first invariant is conserved by the transport process. The data coverage consisted of nine radial bins in the range $L = 3$ – 7 and 30μ bins in the range 0.1–100 keV/nT. Forty to fifty measurements were averaged for most bins.

Figure 1 shows radial profiles of the H^+ ion distribution function from the quiet-interval analysis for four selected values of μ . The CRRES solar maximum data (solid diamonds) are compared with the AMPTE/CCE solar minimum observations (open triangles) and the model phase-space densities (solid curves) taken from Sheldon and Hamilton [9]. The shapes of the radial profiles derived from the two spacecraft data sets are strikingly similar, but the absolute level of the H^+ phase-space densities from CRRES exceed those from AMPTE/CCE observations by a factor of 2–3. The CRRES measurements tend to confirm the result of the CCE analysis in showing an excess of phase-space density below $L = 4$ compared to the model.

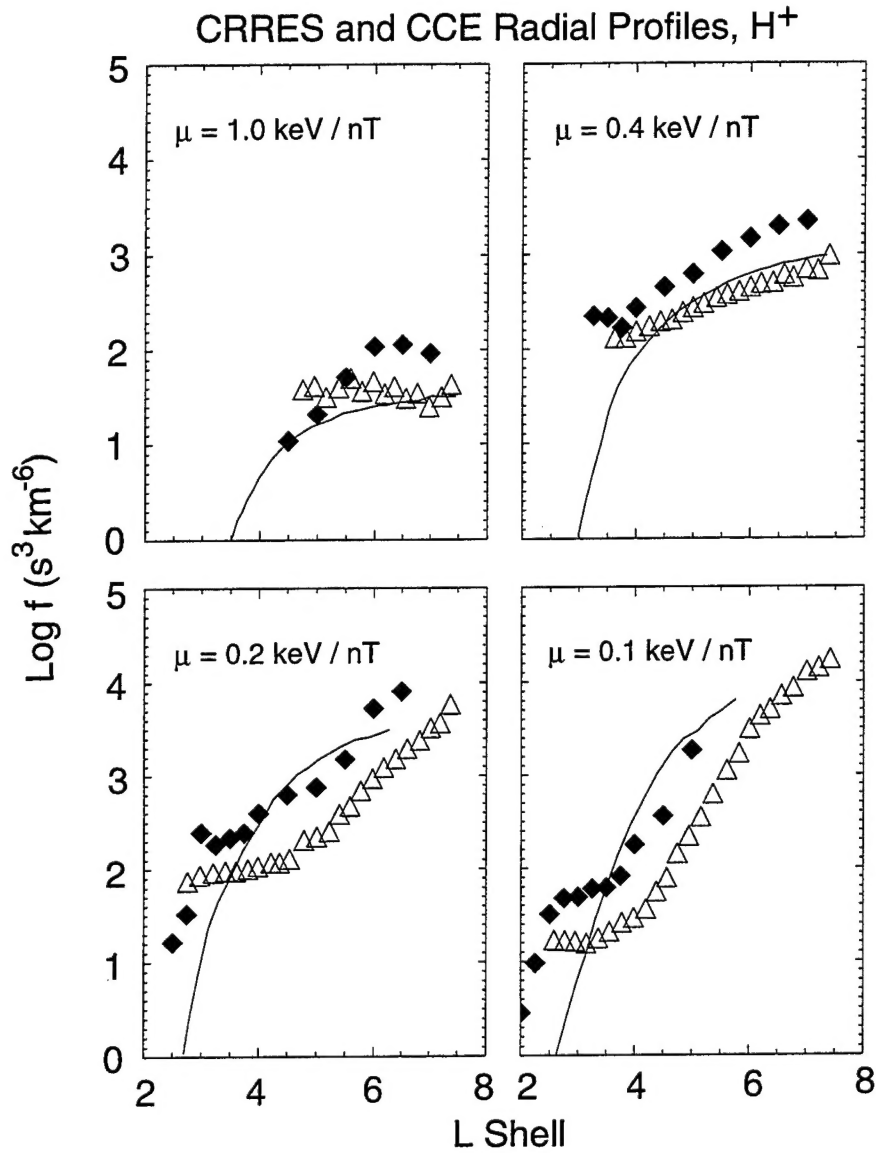


Figure 1. Equatorial radial phase-space density profiles for trapped protons during quiet times at four values of magnetic moment. Observations from the MICS instrument on CRRES are shown as solid diamonds. Similar data from the AMPTE/CCE satellite and the model distributions /9/ are marked as open triangles and curves, respectively.

The model phase-space densities in Figure 1 were computed by numerically solving /9/ the transport equation with standard radial diffusion, charge exchange, and Coulomb drag terms. The outer boundary condition was based on the average AMPTE/CCE spectra at $L \sim 7.4\text{--}7.6$. A non-linear, interactive scheme was used to optimize the parameters of the model in order to best fit the data /9/. Significant differences were found between the observed distributions and the model

results of Figure 1. Sheldon /10/ has successfully modeled the excess of flux at low L shells by invoking enhanced radial diffusion. He suggested that the enhanced radial diffusion was due to the temporal variation of ionospheric electric fields mapped upward into the magnetosphere.

Similar plots of the radial profiles of the He^+ and He^{++} distributions during quiet times are shown in Figures 2 and 3, respectively. The CRRES He^{++} data at high μ overlap the corresponding CCE observations to within a factor of 2. At lower μ values, the He^{++} energy is too low to be counted in the channels used for this analysis. The He^+ ion profiles from CRRES shown in Figure 3 have similar shapes to the CCE profiles but show significantly lower values of f at $L > 5$. This difference seems to deepen for decreasing μ . Future work will extend the profiles to lower μ values by using additional MICS data channels. In general, the CRRES observations lend support to the AMPTE/CCE measurements and model results during quiet times /9,10/, but indicate that there may be reduced He^+ fluxes during solar maximum.

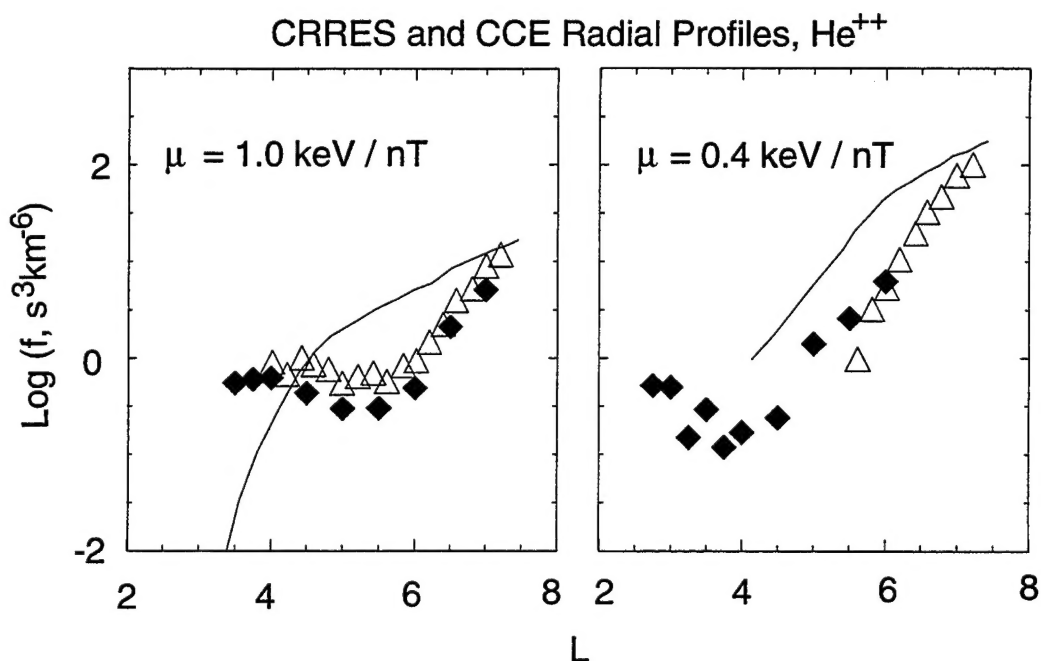


Figure 2. Quiet-time radial profiles of the He^{++} phase-space density at two values of magnetic moment from CRRES and CCE measurements and the standard transport model.

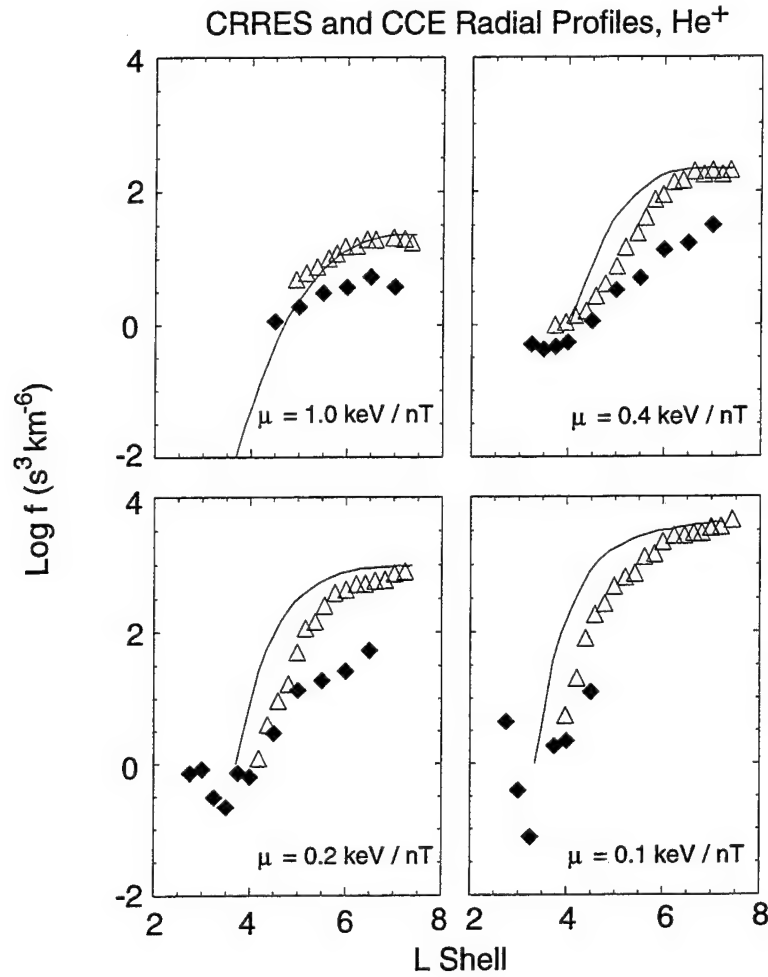


Figure 3. Quiet-time radial profiles of the He^+ phase-space density at four values of magnetic moment from CRRES and CCE measurements and the standard transport model.

Storm-Time Variations of Ion Composition

There was one extremely large magnetic storm and many smaller events during the CRRES mission. The variation of ion composition measured by the CRRES MICS instrument has been studied for several of these storms and compared with similar data taken by the AMPTE/CCE satellite [4,5,6]. Figure 4 shows the Dst index (lower panel) and the total ion energy density in the energy range 40–426 keV at $L = 3$ –5 during the large storm of 23 March 1991 (upper panel). The magnetic local time of apogee of the CRRES spacecraft during this period was approximately 22 hr, and so the data range from local dusk to midnight. This event was an extremely large storm (Dst value -314 nT) comparable in intensity, but of shorter duration than the “great” storm in February 1986 [6]. The data were restricted to the near-equatorial region by

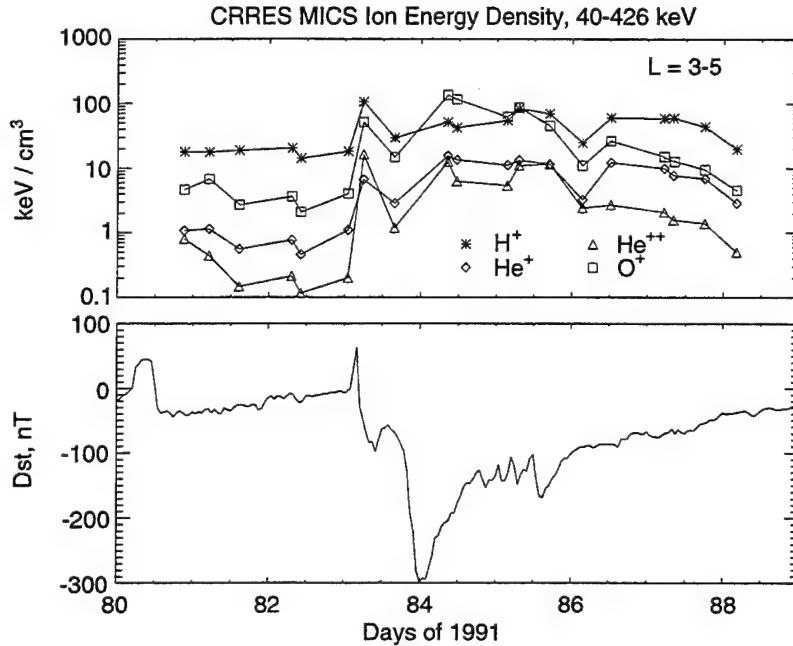


Figure 4. Total ion energy density for $L = 3$ to 5 for the four major ion species in the energy range 40–426 keV compared with the variation of the magnetic index Dst during the large geomagnetic storm on 23 March 1991.

limiting $B/B_0 < 1.2$. This procedure caused the data gaps in the energy density at the beginning of Days 84 and 85.

Prior to the storm on Days 80–82 (March 20–22), the composition was dominated by hydrogen. At approximately 1200 UT on Day 83, the interplanetary shock hit the magnetosphere, causing the sharp positive spike in Dst and the corresponding pulse of ions. This compressive ion enhancement had approximately the same relative composition as the pre-storm distribution and reflects a partially adiabatic response to the magnetospheric compression associated with the SSC. By the middle of Day 83, this transient had subsided to the pre-storm levels. Note that the Dst index during this transient showed only a moderate depression, suggesting that the intense pulse of ions was local, and thus, not a global enhancement of the ring current. This feature swiftly disappeared as the compression of the magnetosphere was removed. Some fraction of the ions represented in the initial enhancement may have been pseudo-trapped, forming a partial ring current that drifted rapidly away.

Near the time of the deep minimum in the Dst index, the relative ion composition at this L shell was dominated by oxygen. This finding is consistent with results of Hamilton and Gloeckler /6/. The hydrogen component initially increased during the recovery phase of the storm, while the oxygen energy density decayed. By Day 86 the hydrogen became dominant, and all the ion populations continued to decay to pre-storm levels. Variations in the helium populations tended to follow the same general temporal profile as the hydrogen ions. Some of the short-term varia-

tions in ion energy densities may have been due to magnetic-latitude variations in the CRRES orbit. (Because of the 18° inclination of the CRRES orbit, it is very difficult to eliminate magnetic-latitude effects from the observed temporal variations without eliminating all the data. No effort has been made to map the fluxes to the magnetic equator by using observed or modeled pitch-angle distributions. The results of this more difficult analysis will be presented in a later paper.) The same general behavior was observed at $L = 5-7$ but with some additional short-term temporal variations. The hydrogen component tended to dominate in the higher L bin by a large factor, except during the peak of the main phase of the storm. The relative contribution of He^{++} to the total ion population was larger at higher L values than lower L values during the recovery phase. This feature may reflect conversion of a solar wind He^{++} source to He^+ by charge exchange as the ions are transported to lower L shells.

The CRRES observations during the large storm of March 1991 are thus qualitatively similar to other large storms, such as those reported by Hamilton and Gloeckler /6/. The oxygen contribution to the ring-current energy density in the CRRES data became dominant by approximately a factor of 3 over the other measured ion species. However, the CRRES mission occurred during solar maximum, whereas the AMPTE/CCE data were taken at solar minimum. It is well established that oxygen-ion outflow from the auroral ionosphere increases by an order of magnitude from solar minimum to solar maximum /15/. This variation could easily account for the small differences in relative composition found between the CCE and CRRES observations.

The faster decay of the oxygen ion component leads back to a proton-dominated ring current at the break in the *Dst* recovery on Day 85. The decay rates before and after the break were qualitatively consistent with the loss rates due to charge exchange for O^+ and H^+ , respectively. Figure 4 thus lends further support to the conclusion of Hamilton and Gloeckler /6/ that the two-stage recovery of *Dst* in large storms is due to change in relative ion composition. However, we note that many of the more moderate storms had proton-dominated ring currents and still exhibited the two-stage signature in the *Dst* profile. A comprehensive study of this question, using the CRRES ion observations during several storms, will be presented in a future paper.

A crude integration of the ion energy density was performed for comparison with *Dst* in order to test the Dessler-Parker-Sckopke relation /16,17/. The calculation was similar to that done by Hamilton and Gloeckler /6/. The total energy content of the ring current population was calculated for the three L shell ranges 2-3, 3-5, and 5-7. This was done by summing the average energy densities for the various species in each L interval. The total ion energy densities that resulted were multiplied by the corresponding flux-tube volumes, and then summed to arrive at a total particle energy for the ring current. (This procedure assumes symmetry in local time.) The total energy is then converted by the Dessler-Parker-Sckopke relation into a predicted perturbation field that is compared with *Dst*. For example, at approximately 1200 UT on Day 85, the *Dst* index was -185 nT, whereas the predicted perturbation from the particle measurements was -94 nT. This analysis shows that the measured fluxes in the March 1991 storm could account for only 30-50% of the measured variation of *Dst*. Hamilton and Gloeckler /6/ had accounted for 24-84% of the observed *Dst* variation during the February 1986 storm with energy content deduced from AMPTE/CCE data, but they noted several assumptions in their calculation that could have led to uncertainty in the prediction. Part of their discrepancy may have been due to the assumption of an azimuthally symmetric ion population. However, the dusk-midnight local

time position of CRRES should result in an overestimate of the particle contribution because of the dusk-side partial ring current. Both calculations also assumed particle isotropy, which means that the CRRES estimate should provide an upper limit on the total energy of the ring current.

Conclusions

Observations from the MICS instrument on the CRRES spacecraft yield results qualitatively similar to those of the AMPTE/CCE mission. During geomagnetically quiet intervals, CRRES observed ion phase-space densities with radial profiles similar to those observed by the AMPTE/CCE mission. The CRRES profiles are similar to those that led Sheldon /10/ to invoke diffusion by electric-field variations of ionospheric origin to enhance the transport the ions down to low L shells. However, the relative compositions observed by CRRES near solar maximum were different from those detected by CCE at solar minimum: the H^+ densities were larger in the CRRES data than in the AMPTE/CCE data by a factor of 2–3, and the He^+ densities were smaller by about the same factor. Some of these differences may reflect changes in the source intensities and the transport processes over the solar cycle. (The He^{++} distribution observed by CRRES was almost exactly equal to that reported from CCE.)

During the large geomagnetic storm of March 1991, CRRES observed composition variations similar to those detected by CCE during a similar large storm. Oxygen ions dominated the other plasma constituents during the March 1991 storm by an even larger factor than that previously observed by CCE. This result is consistent with the increased oxygen outflow from the auroral ionosphere that is typical of the peak of the solar cycle. The change in ion composition (from O^+ to H^+) during recovery phase was well correlated with the observed two-stage recovery of the Dst index. However, this hypothesis /6/ still cannot explain the similar signatures observed in connection with moderate and small storms.

A preliminary calculation was performed to predict the global magnetic field perturbation from the total measured particle energy in the ring current. It was found that the observed particle fluxes could account for only 30–50% of the variation in Dst observed during the March 1991 storm. This discrepancy between the ion observations and the Dst hints that there may be important contributions to Dst in addition to the ring current /18/. Other criticisms of the Dessler-Parker-Sckopke model have been noted, for example, it's inclusion of a self-energy term for the ring current /19/. Future work will include a more detailed comparison of the CRRES data with this model for several geomagnetic storms.

References

1. L. A. Frank and H. D. Owens, Omnidirectional intensity contours of low-energy protons ($0.5 \text{ keV} < E < 50 \text{ keV}$) in the Earth's outer radiation zone at the magnetic equator, *J. Geophys. Res.*, 75, 1269 (1970).
2. D. J. Williams, Phase-space variations of near equatorially mirroring ring current ions, *J. Geophys. Res.*, 86, 189 (1981).
3. D. J. Williams and M. Sugiura, The AMPTE charge composition explorer and the 4-7 September 1984 geomagnetic storm, *Geophys. Res. Lett.*, 12, 305 (1985).
4. G. Gloeckler, B. Wilken, W. Stüdemann, F. M. Ipavich, D. Hovestadt, D. C. Hamilton, and G. Kremser, First composition measurement of the bulk of the storm-time ring current (1 to 300 keV/e) with AMPTE/CCE, *Geophys. Res. Lett.*, 12, 325 (1985).
5. S. M. Krimigis, G. Gloeckler, R. W. McEntire, T. A. Potemra, F. L. Scarf, and E. G. Shelley, Magnetic storm of September 4, 1984: a synthesis of ring current spectra and energy densities measured with AMPTE/CCE, *Geophys. Res. Lett.*, 12, 329 (1985).
6. D. C. Hamilton and G. Gloeckler, Ring current development during the great geomagnetic storm of February 1986, *J. Geophys. Res.*, 93, 14343 (1988).
7. B. A. Tinsley, Evidence that the recovery phase ring current consists of helium ions, *J. Geophys. Res.*, 81, 6193 (1976).
8. L. R. Lyons and D. S. Evans, The inconsistency between proton charge exchange and the observed ring current decay, *J. Geophys. Res.*, 81, 6197 (1976).
9. R. B. Sheldon and D. C. Hamilton, Ion transport and loss in the Earth's quiet ring current, 1. Data and standard model, *J. Geophys. Res.*, 98, 13491 (1993).
10. R. B. Sheldon, Ion transport and loss in the Earth's quiet ring current, 2. diffusion and magnetosphere ionosphere coupling, *J. Geophys. Res.*, 99, 5705 (1994).
11. W. N. Spjeldvik, Equilibrium structure of equatorially mirroring radiation belt protons, *J. Geophys. Res.*, 82, 2801 (1977).
12. M. H. Johnson and J. Kierein, Combined Release and Radiation Effects Satellite (CRRES): spacecraft and mission, *J. Spacecraft and Rockets*, 29, 556 (1992).
13. B. Wilken, W. Weiss, D. Hall, M. Grande, F. Sørass, and J. F. Fennell, Magnetospheric ion composition spectrometer onboard the CRRES spacecraft, *J. Spacecraft and Rockets*, 29, 585 (1992).
14. R. Koga, S. S. Imamoto, N. Katz, and S. D. Pinkerton, Data processing units for eight magnetospheric particle and field sensors, *J. Spacecraft and Rockets*, 29, 574 (1992).

15. A. W. Yau, E. G. Shelley, W. K. Peterson, and L. Lenchyshyn, Energetic auroral and polar ion outflow at DE 1 altitudes: magnitude, composition, magnetic activity dependence, and long-term variations, *J. Geophys. Res.*, 90, 8417 (1985).
16. A. J. Dessler, and E. N. Parker, Hydromagnetic theory of geomagnetic storms, *J. Geophys. Res.*, 64, 2239 (1959).
17. N. Sckopke, A general relation between the energy of trapped particles and the disturbance field over the Earth, *J. Geophys. Res.*, 71, 3125 (1966).
18. W. H. Campbell, Geomagnetic storms, lognormal distributions, and the *Dst* ring-current myth, *J. Geophys. Res.*, in press (1995).
19. R. L. Carovillano and G. L. Siscoe, Energy and momentum theories of magnetospheric processes, *Rev. Geophys.*, 11, 289 (1973).

TECHNOLOGY OPERATIONS

The Aerospace Corporation functions as an "architect-engineer" for national security programs, specializing in advanced military space systems. The Corporation's Technology Operations supports the effective and timely development and operation of national security systems through scientific research and the application of advanced technology. Vital to the success of the Corporation is the technical staff's wide-ranging expertise and its ability to stay abreast of new technological developments and program support issues associated with rapidly evolving space systems. Contributing capabilities are provided by these individual Technology Centers:

Electronics Technology Center: Microelectronics, solid-state device physics, VLSI reliability, compound semiconductors, radiation hardening, data storage technologies, infrared detector devices and testing; electro-optics, quantum electronics, solid-state lasers, optical propagation and communications; cw and pulsed chemical laser development, optical resonators, beam control, atmospheric propagation, and laser effects and countermeasures; atomic frequency standards, applied laser spectroscopy, laser chemistry, laser optoelectronics, phase conjugation and coherent imaging, solar cell physics, battery electrochemistry, battery testing and evaluation.

Mechanics and Materials Technology Center: Evaluation and characterization of new materials: metals, alloys, ceramics, polymers and their composites, and new forms of carbon; development and analysis of thin films and deposition techniques; nondestructive evaluation, component failure analysis and reliability; fracture mechanics and stress corrosion; development and evaluation of hardened components; analysis and evaluation of materials at cryogenic and elevated temperatures; launch vehicle and reentry fluid mechanics, heat transfer and flight dynamics; chemical and electric propulsion; spacecraft structural mechanics, spacecraft survivability and vulnerability assessment; contamination, thermal and structural control; high temperature thermomechanics, gas kinetics and radiation; lubrication and surface phenomena.

Space and Environment Technology Center: Magnetospheric, auroral and cosmic ray physics, wave-particle interactions, magnetospheric plasma waves; atmospheric and ionospheric physics, density and composition of the upper atmosphere, remote sensing using atmospheric radiation; solar physics, infrared astronomy, infrared signature analysis; effects of solar activity, magnetic storms and nuclear explosions on the earth's atmosphere, ionosphere and magnetosphere; effects of electromagnetic and particulate radiations on space systems; space instrumentation; propellant chemistry, chemical dynamics, environmental chemistry, trace detection; atmospheric chemical reactions, atmospheric optics, light scattering, state-specific chemical reactions and radiative signatures of missile plumes, and sensor out-of-field-of-view rejection.